

Study on Cyclic Constitutive Model and Ultra Low Cycle Fracture Prediction Model of Duplex Stainless Steel

Speaker: Xiao Chang

Research group: Xiao Chang: Beijing University of Technology, Beijing, China
Lu Yang*: Beijing University of Technology, Beijing, China
Liang Zong: School of Civil Engineering, Tianjin, Beijing, China
Meng-Han Zhao: Beijing University of Technology, Beijing, China
Fei Yin: Beijing University of Technology, Beijing, China

Contents

1. Background

2. Constitutive Model

3. Fracture Prediction Model

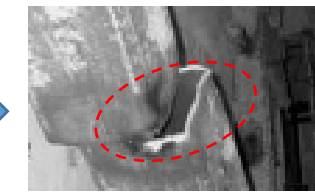
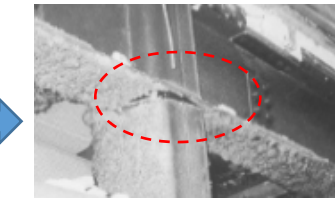
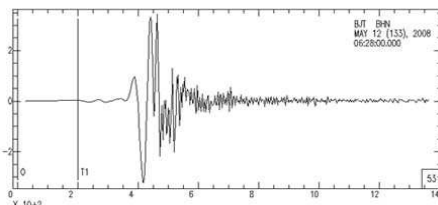
4. Conclusion



1. Background



1. Background



Seismic event
Large strain ultra low cyclic

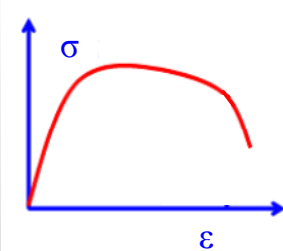
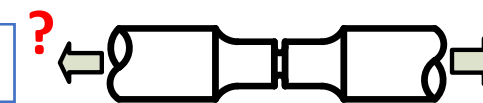
Structural members
(dissipative elements)

Crack initiation

Fracture



J integral criterion



Ductile fracture problem without
obvious defects and occurred with
large scale yielding



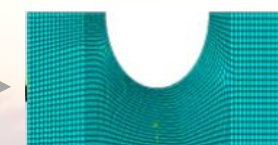
Elongation

Cyclic constitutive model



Elongation

Monotonic constitutive model



Finite element
subroutine

FEA subroutine
back-calculate

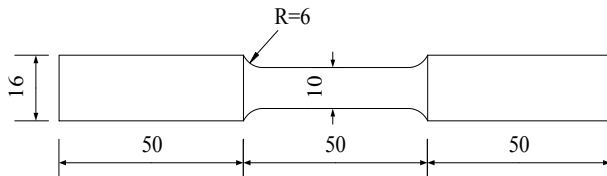
VGM,SMCS,CVGM Fracture Prediction Model



2. Constitutive Model

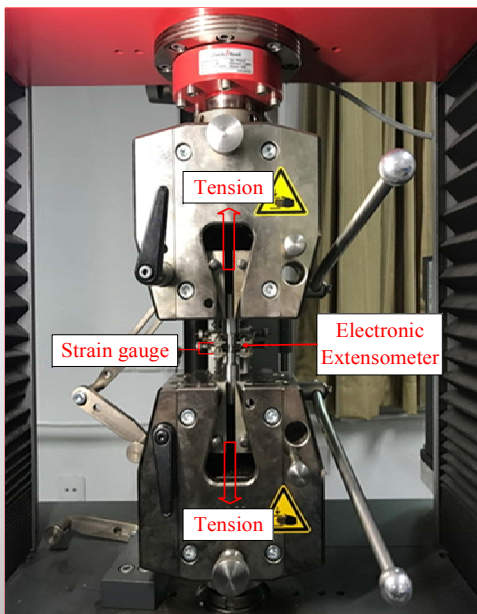


2.1 smooth round bar test

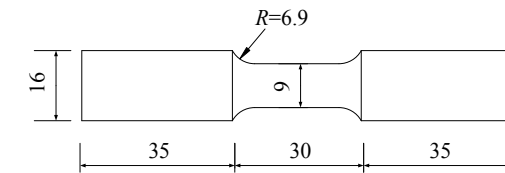


Monotonic loading

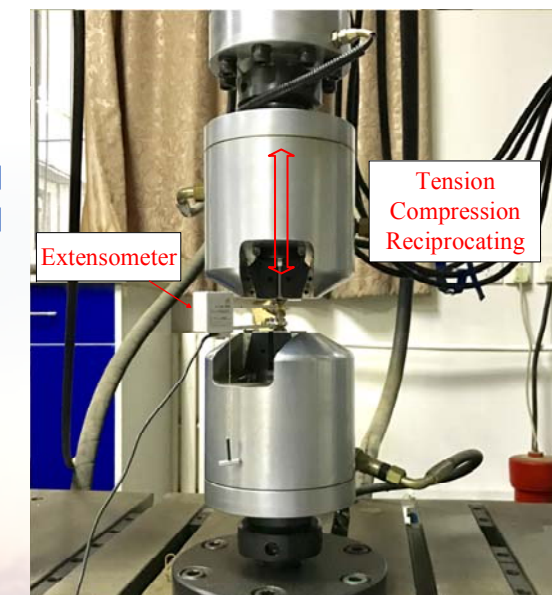
- Duplex stainless steel S220503 (ASTMS31803, EN 1.4462)
- Cut from 16mm thick base material along rolling direction



Monotonic constitutive model



Cyclic loading



Cyclic constitutive model

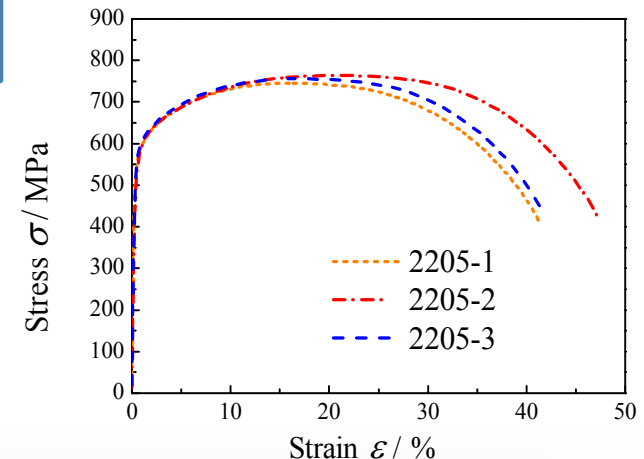
- Electronic universal testing machine

- A servo-hydraulic universal test machine

2.1 smooth round bar test

R-O model modified by Gardner and Nethercot(2004)

$$\varepsilon = \begin{cases} \frac{\sigma}{E_0} + 0.002 \left(\frac{\sigma}{\sigma_{0.2}} \right)^n & \sigma \leq \sigma_{0.2} \\ \frac{\sigma - \sigma_{0.2}}{E_{0.2}} + \left(0.008 - \frac{\sigma_{1.0} - \sigma_{0.2}}{E_{0.2}} \right) \times \left(\frac{\sigma - \sigma_{0.2}}{\sigma_{1.0} - \sigma_{0.2}} \right)^{n_{0.2,1.0}} + \varepsilon_{t,0.2} & \sigma > \sigma_{0.2} \end{cases}$$



| Specimen | E_0 | $\sigma_{0.01}$ | $\sigma_{0.2}$ | $\varepsilon_{0.2}$ | $\sigma_{1.0}$ | σ_u | A | $E_{0.2}$ | n | n' |
|----------|--------|-----------------|----------------|---------------------|----------------|------------|-------|-----------|------|------|
| | [MPa] | [MPa] | [MPa] | [%] | [MPa] | [MPa] | [%] | [MPa] | - | - |
| 2205-1 | 195000 | 297.7 | 519.48 | 47.21 | 611.96 | 763.12 | 47.01 | 38666 | 5.38 | 2.25 |
| 2205-2 | 230000 | 273.3 | 545.71 | 42.62 | 619.03 | 755.07 | 41.79 | 48418 | 4.33 | 2.31 |
| 2205-3 | 254000 | 326.1 | 530.24 | 42.98 | 607.78 | 745.98 | 41.06 | 36758 | 6.16 | 2.32 |
| average | 226000 | 299 | 531.81 | 44.27 | 612.92 | 754.72 | 43.29 | 41614 | 5.29 | 2.96 |

2.1 smooth round bar test

True stress strain

$$\varepsilon_{true} = \ln(1 + \varepsilon_{eng}) \quad \sigma_{true} = \sigma_{eng}(1 + \varepsilon_{eng})$$

necking

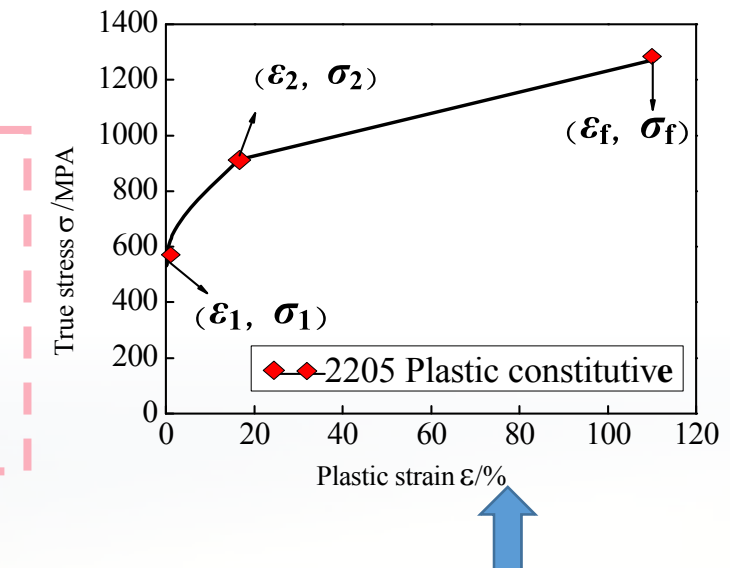
True stress-plastic strain

$$\varepsilon_{pl} = |\varepsilon_{true}| - |\sigma_{true}| / E$$

True stress strain at the fracture point

$$\left\{ \begin{array}{l} \sigma_f = \frac{P_f}{\pi d_f^2 / 4} \\ \varepsilon_f = \ln \left[\left(\frac{d_0}{d_f} \right)^2 \right] \end{array} \right.$$

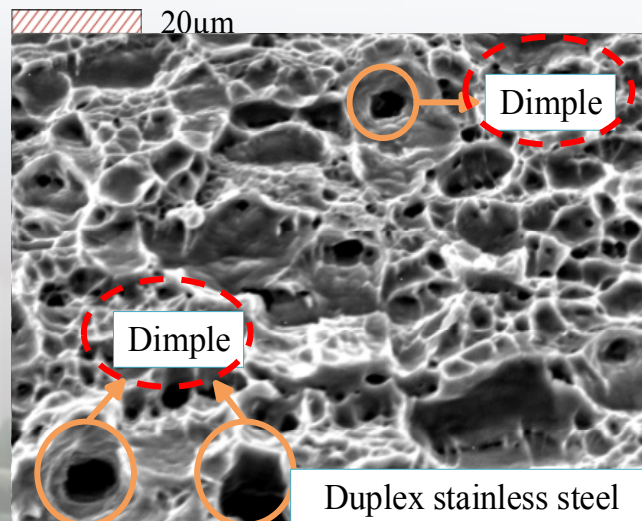
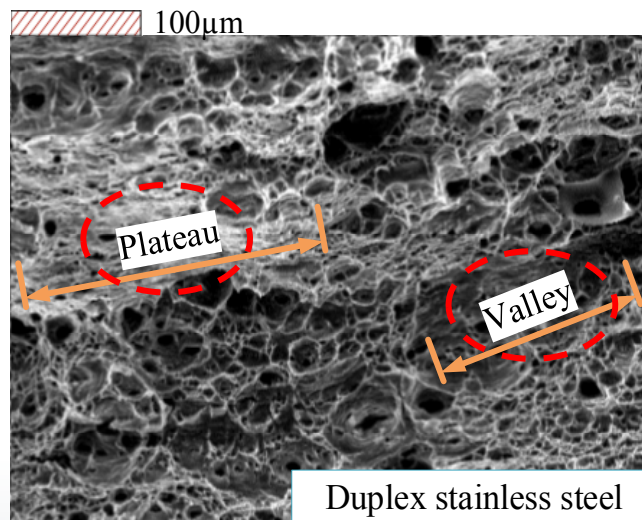
- ❖ The true stress plastic strain with the fracture point are input the Abaqus



Tab. 3 Key parameters of the constitutive model used in FEA based on true stress-strain relationship

| Material | $\sigma_{0.2}$ /MPa | ε_1 /% | σ_1 /MPa | ε_2 /% | σ_2 /MPa | ε_f /% | σ_f /MPa |
|----------|------------------------|-----------------------|--------------------|-----------------------|--------------------|-----------------------|--------------------|
| S220503 | 531.81 | 0.002 | 532 | 0.165 | 912.55 | 1.11 | 1275.40 |

2.1 smooth round bar test

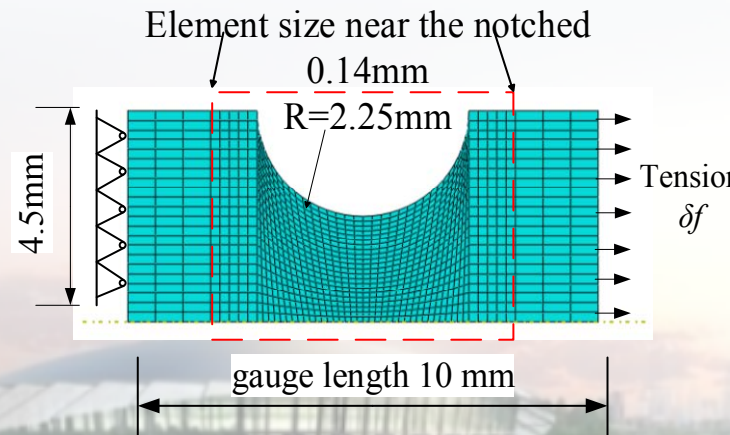


Tab.6 Results of Characteristic length

| Material | Characteristic Length l^*/mm | | |
|----------|---------------------------------------|------------|-------------|
| | Lower Bound | Mean Value | Upper Bound |
| S220503 | 0.01 | 0.136 | 0.214 |

Twice the average **dimple** diameter

Average of ten measurements lengths of the **plateaus and valleys**



The largest plateau or valley

2.2 smooth round bar cyclic test

The loading process is stopped when obvious buckling occurs

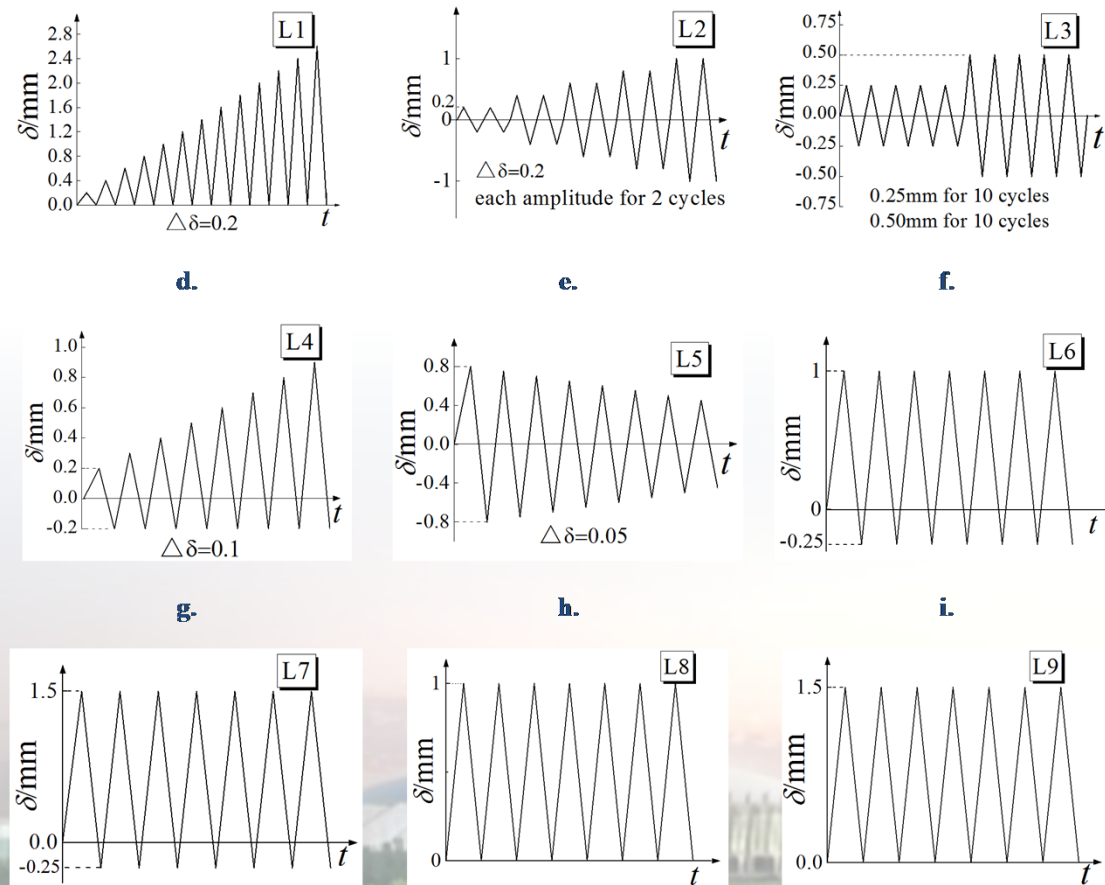


Fig.7 Cyclic loading protocols

2.2 smooth round bar cyclic test

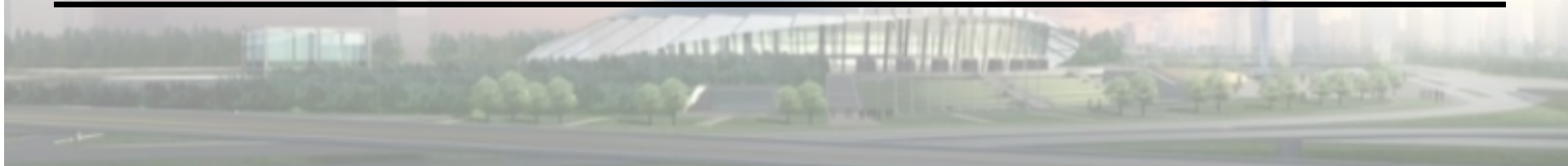
- ✓ The **von Mises flow rule** and **mixed model** combining both isotropic hardening and non-linear kinematic hardening.
- ✓ The **parameters of cyclic hardening** was calibrated from the test data according to the help files of ABAQUS

$$\sigma^0 = \sigma|_0 + Q_\infty [1 - \exp(-b\varepsilon_p)] \longrightarrow [Q_\infty \text{ and } b]$$

$$\alpha = \sum_{k=1}^4 \alpha_k = \sum_{k=1}^4 \frac{C_k}{\gamma_k} [1 - \exp(-\gamma_k \varepsilon_p)] \longrightarrow [C_k \text{ and } \gamma_k]$$

Tab. 4 Calibration parameters of specimens

| Specimen | $\sigma _0$ /MPa | Q_∞ /MPa | b_{iso} | $C_{\text{kin},1}$ /MPa | γ_1 | $C_{\text{kin},2}$ /MPa | γ_2 | $C_{\text{kin},3}$ /MPa | γ_3 | $C_{\text{kin},4}$ /MPa | γ_4 |
|----------|---------------------|--------------------|------------------|----------------------------|------------|----------------------------|------------|----------------------------|------------|----------------------------|------------|
| AVG. | 299 | 62 | 6.6 | 65020 | 662 | 41222 | 417 | 31286 | 319 | 23210 | 249 |



2.2 smooth round bar cyclic test

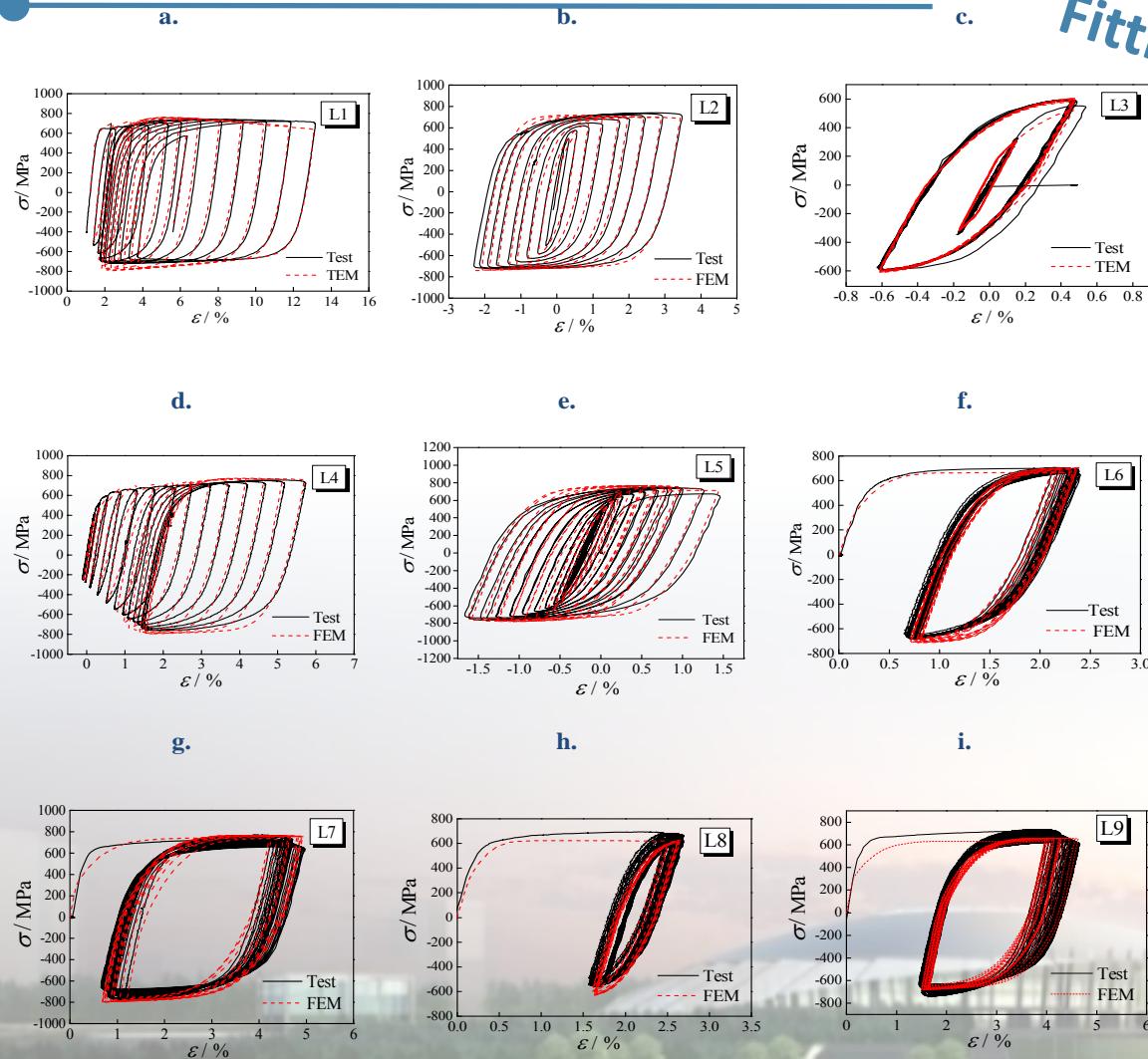


Fig. 8 Stress-strain curves of cyclic loading

Fitting well

✓ The simulated curves **agree well** with test data which means that the **parameters of cyclic loading can be used in the simulation of stainless steel under cyclic loading**.

2.2 smooth round bar cyclic test

- ✓ The response of stainless steel under cyclic loading is different from that under monotonic loading, which can be expressed by **cyclic skeleton curves**.
- ✓ One of the widely used models is **Ramberg-Osgood model**, Eq. 11.

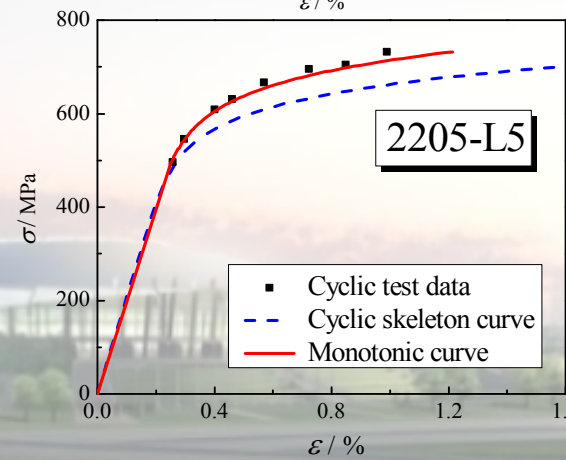
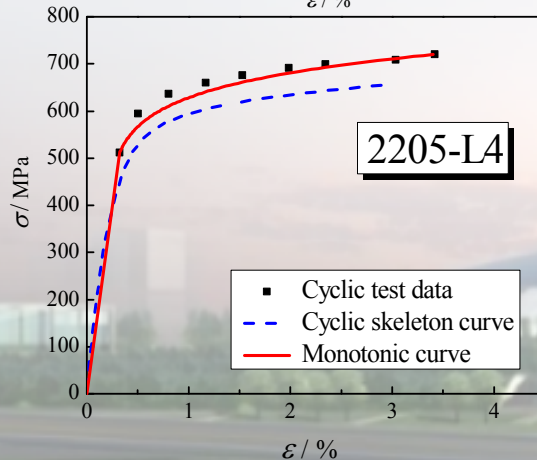
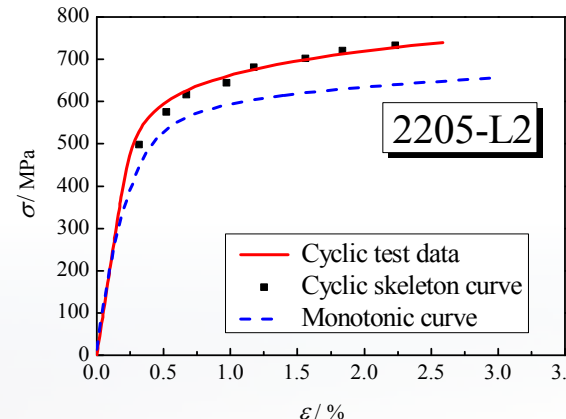
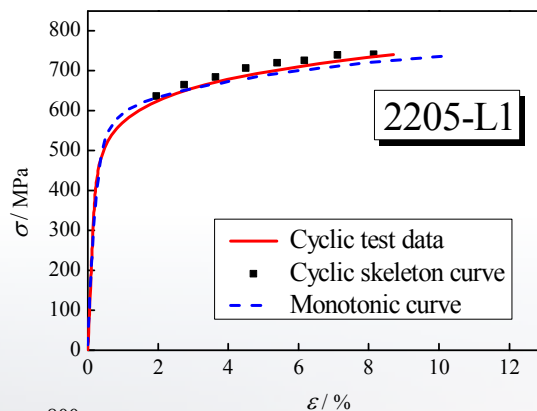
$$\frac{\Delta \varepsilon}{2} = \frac{\Delta \varepsilon_e}{2} + \frac{\Delta \varepsilon_p}{2} = \frac{\Delta \sigma}{2E} + \left(\frac{\Delta \sigma}{2K} \right)^{\frac{1}{n}} \quad (\text{Eq. 11})$$

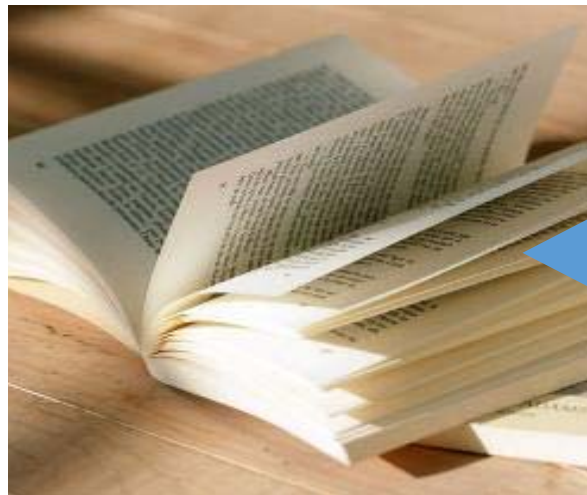
Tab.5 Parameters of the cyclic hardening

| No. of specimen | K'/Mpa | n' |
|-----------------|--------|---------|
| 2205-L1 | 511.5 | 0.09698 |
| 2205-L2 | 560.8 | 0.09267 |
| 2205-L4 | 528.3 | 0.09184 |
| 2205-L5 | 545.7 | 0.09239 |
| AVG. | 536.6 | 0.09347 |

2.2 smooth round bar cyclic test

- ✓ Response of stainless steel : cyclic loading \neq monotonic loading;
- ✓ Ramberg-Osgood model **fits** the cyclic skeleton curves **well**;
- ✓ With the increase of the cyclic loops, **strength increases**, especially in the later stage of cyclic loading.



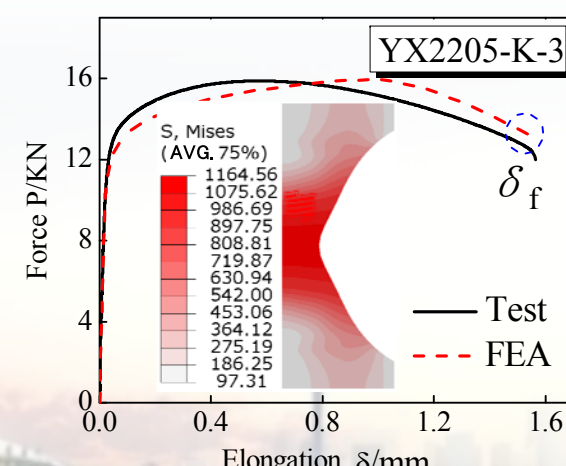
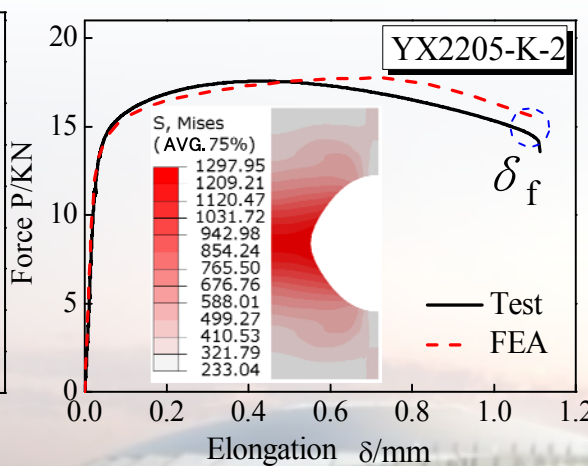
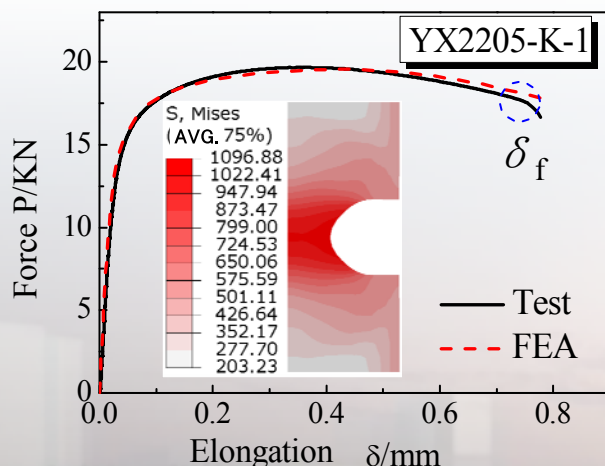
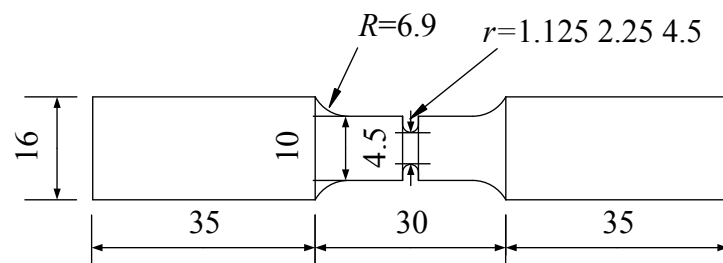


3. Fracture Prediction Model



3.1 notched round bar monotonic test

$$FI_{SMCS} = \varepsilon_p - \gamma \cdot \exp(-1.5T) \geq 0 \quad FI_{VGM} = \int_0^{\varepsilon_p} \exp(1.5T) d\varepsilon_p - \eta_{mon}$$



- ❖ δ_f at the fracture point was the elongation control in FEA
- ❖ through the subroutine, back-calculate the parameters η and γ

3.1 notched round bar monotonic test

Tab.7 Calibrations for toughness parameters of VGM and SMCS models

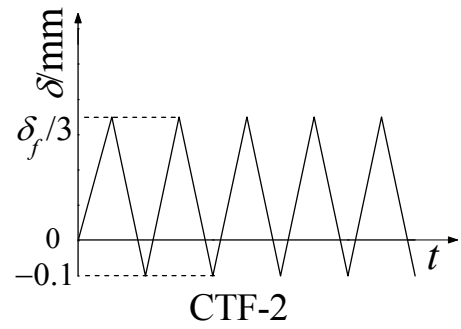
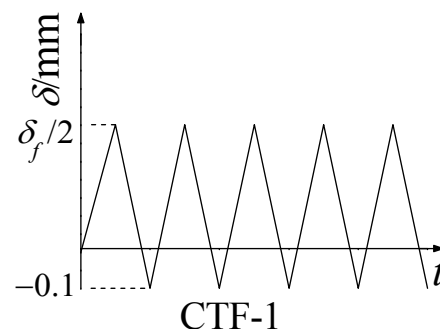
| R /mm | Specimen | δ_f/mm | σ_m /MPa | σ_e /MPa | T | $\varepsilon_{p,cr}$ | γ | η_{mon} |
|----------|------------|---------------|--------------------|--------------------|-------|----------------------|----------|--------------|
| 1.125 | 2205-k-1-1 | 0.73 | 1422 | 1079 | 1.318 | 0.599 | 3.097 | 3.000 |
| | 2205-k-1-2 | 0.78 | 1432 | 1097 | 1.305 | 0.646 | 3.338 | 3.294 |
| 2.25 | 2205-k-2-1 | 1.11 | 1154 | 1106 | 1.043 | 0.669 | 3.137 | 2.998 |
| | 2205-k-2-2 | 1.03 | 1134 | 1081 | 1.046 | 0.604 | 2.843 | 2.686 |
| 4.5 | 2205-k-3-1 | 1.56 | 1047 | 1165 | 0.899 | 0.822 | 3.168 | 2.851 |
| | 2205-k-3-2 | 1.52 | 1031 | 1152 | 0.895 | 0.790 | 3.027 | 2.727 |
| AVG. | | | | | | | 3.101 | 2.926 |
| COV/% | | | | | | | 4.82 | 6.96 |

Both can describe the fracture, and it independent of the geometry and stress state

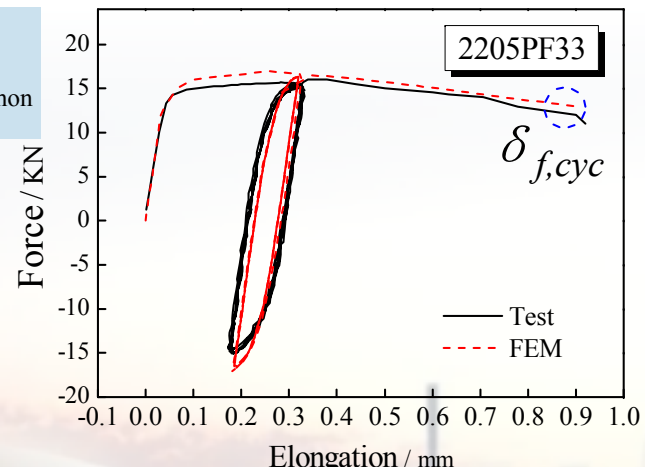
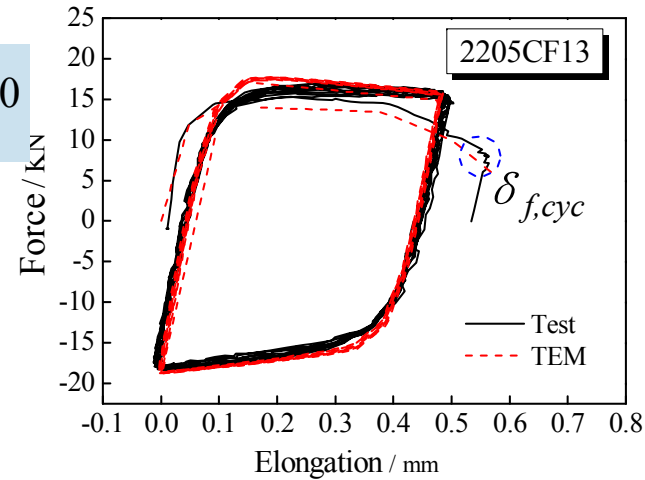
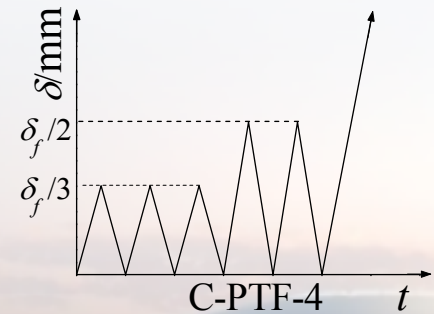
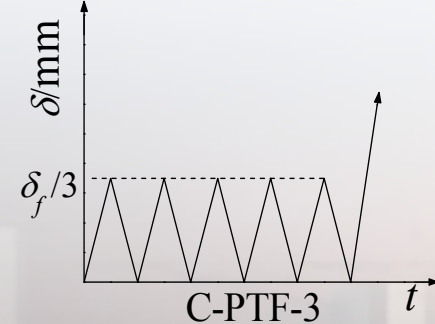
Can be applied to predict the ductile crack initiation of duplex stainless steel

3.2 notched round bar cyclic test

$$VGD_{cyc} = \sum_{\text{tensile}} \int_{\varepsilon_1}^{\varepsilon_2} \exp(|1.5T|) d\varepsilon_p - \sum_{\text{compressive}} \int_{\varepsilon_1}^{\varepsilon_2} \exp(|1.5T|) d\varepsilon_p \geq 0$$



$$\eta_{cyc} = \frac{\ln(r_{cr}/r_0)_{cyc}}{C} = \exp(-\lambda\varepsilon_c) \frac{\ln(r_{cr}/r_0)_{mon}}{C} = \exp(-\lambda\varepsilon_c) \cdot \eta_{mon}$$



- ❖ $\delta_{f,cyc}$ with the cyclic numbers of fracture N_f was input in FEA
- ❖ through the subroutine, back-calculate the parameters λ_{CVGM}

3.2 notched round bar cyclic test

Tab.8 The results of notched round bars under four different loading systems

| R /mm | Loading systems | Specimen | displacement control | N_f | $\delta_{f,cyc}$ /mm | λ_{CVGM} | |
|------------------|--------------------|----------|--|-------|-------------------------|------------------|--|
| 1.125 | CTF | 2205CF11 | 0.447 $\leftarrow\rightarrow$ 0.059 | 3 | 0.376 | 0.435 | |
| | | 2205CF21 | 0.339 $\leftarrow\rightarrow$ 0.114 | 13 | 0.386 | 0.421 | |
| | | 2205PF31 | 0.106 $\leftarrow\rightarrow$ 0.055(5) | 5 | 0.617 | 0.541 | |
| | C-PTF | 2205PF41 | 0.113 $\leftarrow\rightarrow$ 0.059(3) | 5 | 0.622 | 0.550 | |
| | | | 0.189 $\leftarrow\rightarrow$ 0.113(2) | | | | |
| | C-PTF | 2205CF12 | 0.527 $\leftarrow\rightarrow$ 0.081 | 5 | 0.451 | 0.541 | |
| | | 2205CF22 | 0.394 $\leftarrow\rightarrow$ 0.131 | 15 | 0.455 | 0.502 | |
| | | 2205PF32 | 0.205 $\leftarrow\rightarrow$ 0.127(5) | 5 | 0.741 | 0.563 | |
| | | 2205PF42 | 0.181 $\leftarrow\rightarrow$ 0.106(3) | 5 | 0.759 | 0.583 | |
| | | | 0.271 $\leftarrow\rightarrow$ 0.149(2) | | | | |
| | | 2205CF13 | 0.487 $\leftarrow\rightarrow$ -0.006 | 9 | 0.490 | 0.595 | |
| 2.25 | CTF | 2205CF23 | 0.397 $\leftarrow\rightarrow$ 0.096 | 21 | 0.522 | 0.469 | |
| | | 2205PF33 | 0.327 $\leftarrow\rightarrow$ 0.178(5) | 5 | 0.891 | 0.633 | |
| | | | 0.283 $\leftarrow\rightarrow$ 0.124(3) | | | | |
| | C-PTF | 2205PF43 | 0.469 $\leftarrow\rightarrow$ 0.144(3) | 5 | 0.907 | 0.666 | |
| | | | | | | | |
| | | | | | | | |
| AVG. | | | | | | 0.542 | |
| $COV\% = 13.2\%$ | | | | | | | |

Can be applied to predict the ductile crack initiation of duplex stainless steel

λ_{CVGM} of CVGM model is independent of the geometry and stress state

3.2 notched round bar cyclic test

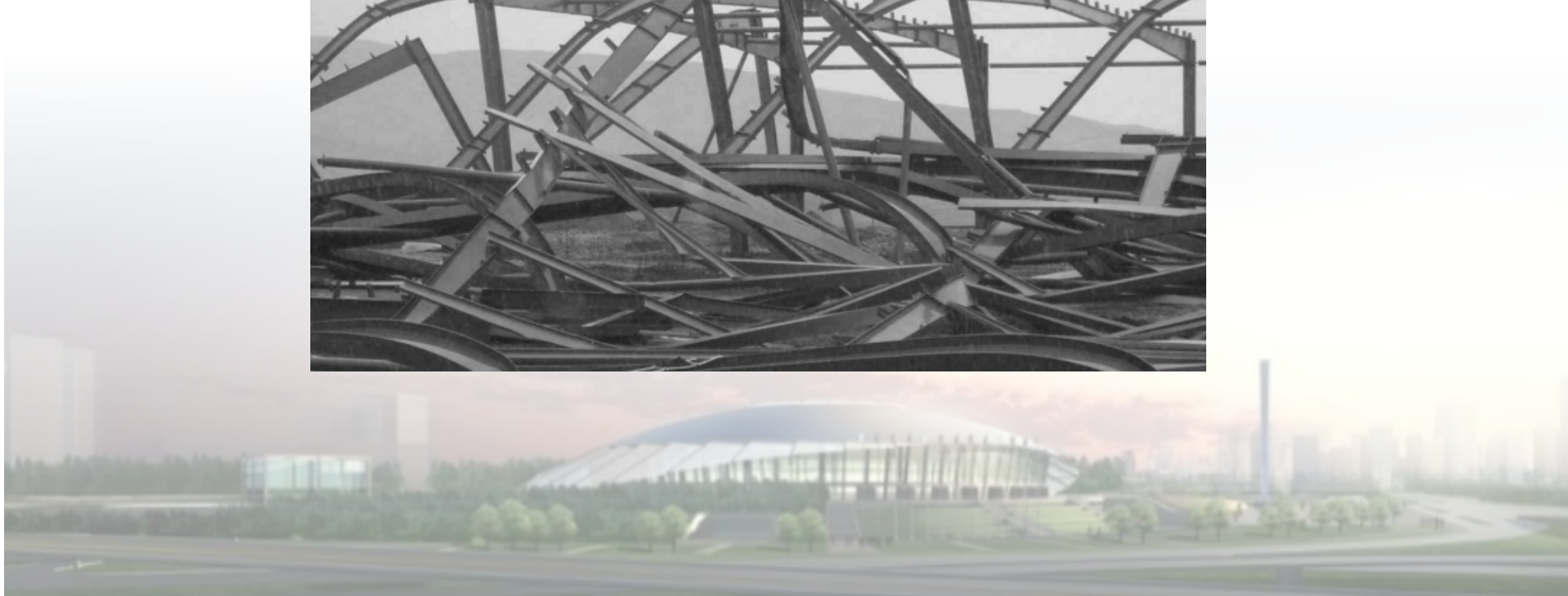
Tab.9 Comparison of micromechanical model parameters of Q345B steel

| Material | $\sigma_{0.2}$ /MPa | σ_u /MPa | $\sigma_{0.2}/\sigma_u$ | A /% | Z /% | d_f/d_0 | γ | η_{mon} | λ_{CVGM} |
|----------------------|------------------------|--------------------|-------------------------|---------|---------|-----------|----------|--------------|------------------|
| S220503 | 532 | 755 | 0.70 | 43.3 | 67.2 | 0.57 | 3.10 | 2.93 | 0.54 |
| Q345 ^[47] | 321 | 522 | 0.64 | 36.2 | 52.1 | 0.53 | 2.53 | 2.82 | 0.26 |

The toughness parameters η_{mon} and γ of duplex stainless steel were both larger than those of Q345, which demonstrates duplex stainless steel has better toughness and comprehensive properties.

[47]Z.H. Jia. Study on damage behavior and calculation model of welded joints of steel frames subjected to strong earthquakes. Beijing University of Technology, 2016.

- ✓ So the three fracture prediction models can predict the crack initiation, which can provide a helpful reference for fracture prediction of duplex stainless steel structures under earthquake condition.





4. Conclusion

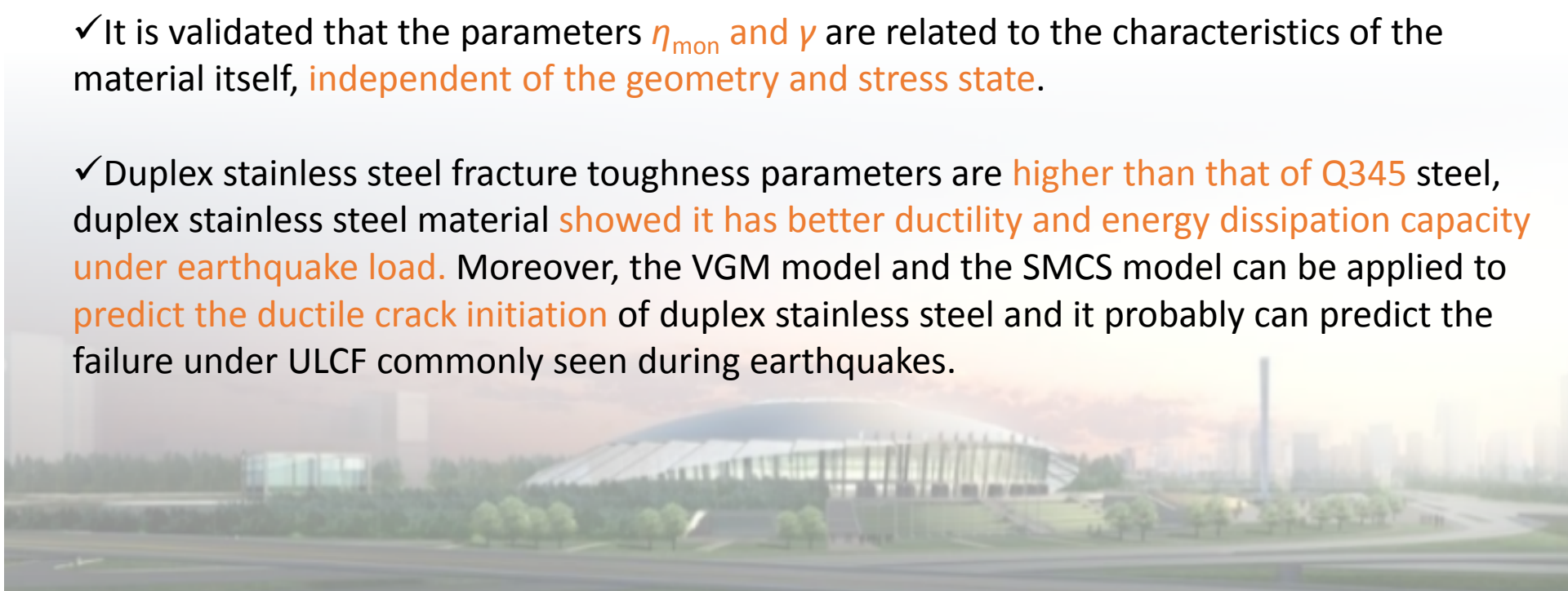


➤ For the cyclic constitutive model part

- ✓ Stainless steel S220503 (ASTM S31803, EN 1.4462) exhibits remarkable nonlinearity; Under cyclic loading, duplex stainless steel exhibits remarkable **cyclic hardening** and **excellent cyclic behavior**;
- ✓ Simulated curves by ABAQUS **agree well** with the test data and **the cyclic hardening parameters** obtained under large strain ultra low cycle in this paper **can be used in the engineering practice**.

➤ For the Ultra Low Cycle Fracture Prediction Model

- ✓ Established the microscopic fracture model VGM, SMCS, CVGM. The Parameters η_{mon} , γ and λ_{CVGM} were calibrated through tensile tests of smooth-notched bars and corresponding FEA which **the parameters can predict the ductile crack initiation** of duplex stainless steel.
- ✓ It is validated that the parameters η_{mon} and γ are related to the characteristics of the material itself, **independent of the geometry and stress state**.
- ✓ Duplex stainless steel fracture toughness parameters are **higher than that of Q345 steel**, duplex stainless steel material **showed it has better ductility and energy dissipation capacity under earthquake load**. Moreover, the VGM model and the SMCS model can be applied to predict the **ductile crack initiation** of duplex stainless steel and it probably can predict the failure under ULCF commonly seen during earthquakes.



Thanks for your attending

